Proceedings of the International MultiConference of Engineers and Computer Scientists 2013 Vol II,
IMECS 2013, March 13 - 15, 2013, Hong Kong

Thermal Response of an Isolated Rectangular, Layered Nickel-Titanium Shape Memory Alloy Thin Film with Variable Material Properties

Mehmet M. Ozturk[1], and Abhijit Bhattacharyya[*2]

***Abstract*—The thermal response of a square SMA island is studied and the results presented in this paper. Based on microstructural studies reported in the literature, the SMA island is taken to have three layers – an amorphous layer, a non-transforming austenite layer and a SMA transforming layer with variable material properties. The spatial as well as the temporal thermal response of the 3-layer island are very close to the thermal response of a single SMA transforming layer island of identical geometry. In either case, the temperatures are significantly lower than those of a SMA layer, infinitely extended over the substrate.**

***Index Terms*—Thermal response, shape memory, thin films**

I. Introduction

Shape memory alloy (SMA) thin films display many of the remarkable abilities of their macroscopic counterparts – these materials undergo a phase transformation and along with it, the films undergo a change in material properties (thermal conductivity, electrical resistivity, heat capacity as well as mechanical properties) and are also capable of displaying reversible transformation strains. Due to these attributes, the films can function as sensors and actuators in the microscale. While the line of research on shape memory thin films is of recent origin [1], the literature on the thermal response of SMA thin films is especially limited.

Recently, Bhattacharyya and Ozturk [2] reported a finite element study of the thermal response of an infinitely extended SMA layer on a substrate. Based on the notion that the microstructure of a thin film is rarely uniform throughout its thickness as well as specific results reported by Lee, Thomas and Rabiei [3], a three layered SMA thin film was used for the modeling – an amorphous layer at the bottom, followed by a non-transforming austenite layer and then a transforming SMA layer. The study incorporated variable material properties of the transforming SMA layer, and compared the thermal response of the 3-layered film with a single layered transforming layer. For an identical current density in both layers, the single layered film typically attained lower temperatures compared to the 3-layered film. This is because the amorphous layer has significantly higher electrical resistivity than either the austenite or martensite, thus contributing to a higher heat source to the 3-layer as compared to the strength of the heat source in the same physical location of the single layered film. While the study is useful as a starting point for understanding the thermal response of SMA thin films, the films in applications are of finite geometric dimensions. Thus, it is important to understand the thermal response of SMA thin film with finite dimensions.

In this paper, we report a study of the thermal response of an isolated rectangular SMA thin film island on a substrate. A three-layered film – an amorphous layer, a non-transforming austenite layer, and a transforming SMA layer – is studied. The transforming SMA layer is taken to have evolving material properties. The response of the 3-layered film is compared with that of a single SMA transformational layer, and the response of different sized films is compared to that of the infinitely extended thin films. The entire computational study is reported in non-dimensional form.

II. THE BOUNDARY VALUE PROBLEM

A. *The dimensional governing equations*

Based on the excellent study of the microstructure of a SMA thin film reported by Lee *et al.*[3], a three-layered film is taken, as shown in Figure 1. The bottom surface is taken to be adiabatic and the rest of the surface of the film(top as well as the sides) are exposed to convective heat transfer; here, "h" is used for the convective heat transfer coefficient. The interfaces between the layers are taken to be thermally perfect. The energy conservation equation is written as [4,5]

$$\vec{\nabla}\left(k_i(T_i)\vec{\nabla}T_i\right)+\rho_i(T_i)J^2 = C_{v,i}(T_i)\frac{\partial T_i}{\partial t} - Hp_i(T_i)\frac{\partial T_i}{\partial t} \tag{1}$$

where $k_i(T_i)$, $\rho_i(T_i)$ and $C_{v,i}(T_i)$ are the thermal conductivity, electrical resistivity and the heat capacity of the i*th* layer respectively. The parameter, H, represents the latent heat of phase transformation. Here, the layers are numbered 1 through 3 from the bottom to the top respectively. In particular, the properties of the amorphous layer (Layer 1) are denoted as $k_1(T_1)=k_{Amor}$, $\rho_1(T_1)=\rho_{Amor}$ and $C_{v,1}(T_1)=C_{v,Amor}$. The properties of the non-transforming austenite layer (Layer 2) are taken as $k_2(T_2)=k_{Aus}$, $\rho_2(T_2)=\rho_{Aus}$ and $C_{v,2}(T_2)=C_{v,Aus}$. The properties of the SMA transforming layer (Layer 3) are taken as $k_3(T_3)=k_{Aus}+\xi(T_3)(k_{Mar}-k_{Aus})$, $\rho_3(T_3)=\rho_{Aus}+\xi(T_3)(\rho_{Mar}-\rho_{Aus})$ and $C_{v,3}(T_3)=C_{v,Aus}+\xi(T_3)(C_{v,Mar}-C_{v,Aus})$ where the subscripts "Aus" and "Mar" refer to

Manuscript received December 25, 2012; revised Jan 31, 2013.
M.M.Ozturk and A. Bhattacharyya are with Department of Systems Engineering, University of Arkansas at Little Rock, Little Rock, AR 72204-1099, USA e-mails:mmozturk@ualr.edu , *[2]axbhattachar@ualr.edu

the austenite and martensite phases respectively. The symbol, ξ, represents the martensite volume fraction that takes values between 0 (pure austenite) and 1 (pure martensite) and is represented by a sigmoidal function. During the austenite to martensite transformation starting and finishing at the temperatures, M_s and M_f, respectively, this function is taken as $\xi(T_3) = 1 - 1/\left(1 - e^{-[T_3-(M_s+M_f)/2]}\right)$ whereas during the martensite to austenite transformation starting and finishing at A_s and A_f respectively, the M_s and M_f in the aforementioned function are replaced by A_s and A_f. Finally, the functions $p_i(T_i)$ (last term in Eq.1) are defined as $p_1(T_1)=0$, $p_2(T_2)=0$ and $p_3(T_3)= \partial\xi/\partial T_3$. The thickness of the *i*th layer is taken as L_i and the in-plane dimension (length or breadth) of the square island (Figure 1) is taken as "w". The ambient temperature is taken as T_0.

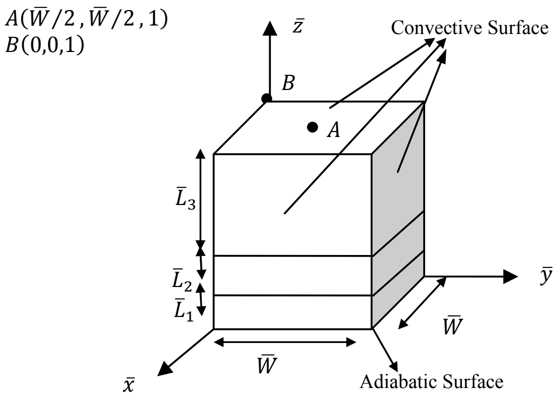

Figure 1. Schematic representation of the boundary value problem where $\bar{L}_1$is Amorphous layer, $\bar{L}_2$ is non-transforming Austenite layer, $\bar{L}_3$ is Transforming SMA layer

B. Nondimensionalization

The computational study is best done after nondimensionalizing the governing equations [2], where the nondimensional counterpart of a dimensional quantity is indicated with an overbar. Defining the total thickness of the SMA film as $L = \sum_{i=1}^{3} L_i$, the temperature field, T_i, and a typical length dimension, e.g. x, are nondimensionalized as

$$\bar{T}_i = T_i/T_0 - 1 \text{ and } \bar{x} = x/L \tag{2}$$

respectively. With these basic nondimensionalized quantities and the governing equations, the following nondimensional quantities emerge naturally from the normalization process:

$$\bar{t} = \frac{k_{Mar}}{L^2 C_{v,Mar}} t, \quad \bar{J} = L\sqrt{\frac{\rho_{Mar}}{T_0 k_{Mar}}} J, \quad \bar{p}_i(\bar{T}_i) = p_i(T_i) T_0,$$

$$\bar{H} = \frac{1}{C_{v,Mar} T_0} H, \quad \bar{h} = \frac{L}{k_{Mar}} h, \quad \bar{k}_i(\bar{T}_i) = \frac{1}{k_{Mar}} k_i(T_i),$$

$$\bar{\rho}_i(\bar{T}_i) = \frac{1}{\rho_{Mar}} \rho_i(T_i), \quad \bar{C}_{v,i}(\bar{T}_i) = \frac{1}{C_{v,Mar}} C_{v,i}(T_i) \quad . \tag{3}$$

III. THE COMPUTATIONAL RESULTS

The material properties of the amorphous layer as well as the austenite and martensite are summarized here. The reader is referred to our first paper [2] on this subject for the details based on how the properties of the amorphous layer were determined. The properties of austenite and martensite are k_{Aus} =28 W/mK, ρ_{Aus}=8.371 x $10^{-4}\Omega$.mm and $C_{v,Aus}$ =5.92 x 10^6 J/Km^3, k_{Mar} =14 W/mK , ρ_{Mar}=9.603 x $10^{-4}\Omega$.mm and $C_{v,Mar}$ =4.50 x 10^6 J/Km^3 [4]. The properties of the amorphous layer are estimated as k_{Amor} =8.90176 W/mK, ρ_{Amor} =12.24508 x $10^{-4}\Omega$.mm and $C_{v,Amor}$ =5.901618 x 10^6 J/Km^3 [2]. The transformation temperatures have been taken as M_f=323 ^{0}C , M_s = 333 ^{0}C , A_s = 345 ^{0}C and A_f = 355 ^{0}C . The ambient temperature has been taken as T_0 = 293 ^{0}C . Based on the work of Lee *et al*.[3], we take the thicknesses of the three layers to be L_1 = 0.2 μ, L_2 = 0.5 μ and L_3 = 1 μ. The convection coefficient was taken as $h = 2\times10^7$ W/m^2.

The computational results are summarized in Figures 2 through 5, all in their nondimensional form. The commercial finite element software, ANSYS, was used with SOLID 70 elements. In our prior work on infinitely extended SMA layers [2], it was determined that a total of 30 elements along the vertical dimension (10 elements of equal thickness in each layer) and a nondimensional time increment, $\Delta\bar{t} = 0.005$, optimally captured the temperature field. We will use the same values here. In addition, we present in Figure 2 the temperature vs. time response for two different locations on the SMA layer (A and B; see Figure 1) for two different numbers of equi-sized square elements in the plane of the SMA layer: 2x2 (or 4 elements) and 4x4 (16 elements). While the difference is certainly noticeable, it is lower for the location at A as compared to the thermal response at B. Since the location at B is more exposed to convective effects than at A, the temperature at the former location is quite a bit lower.

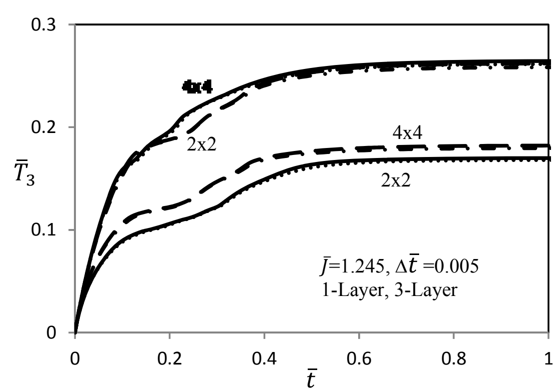

Figure 2. Temperature evolution in three-layer and single layer thin film with respect to time at two different locations -A & B- for different mesh structure.

Also included is the response of the single SMA transforming layer, and the reader will notice that the difference between the thermal response of the 3-layer and the 1-layer model (dotted lines) at the two chosen locations is barely noticeable. In Figures 3 through 5, we present

ISBN: 978-988-19252-6-8
ISSN: 2078-0958 (Print); ISSN: 2078-0966 (Online)

results for a SMA layer with 16 equi-sized square elements in its plane.

The Figure 3 displays the temperature-time response for different sizes of a single SMA transforming layer in its plane. Three different in-plane sizes are included, i.e. $\overline{w} = 0.5, 1$ and 1.5. The temperatures at both locations A and B (Figures 3(a) and (b) respectively) are progressively higher with a larger in-plane film size but in all cases, the temperatures are far lower than the temperature of the infinitely extended layer. This is no doubt because of the vanishing heat flux along the infinitely extended plane of the film.

LOCATION A

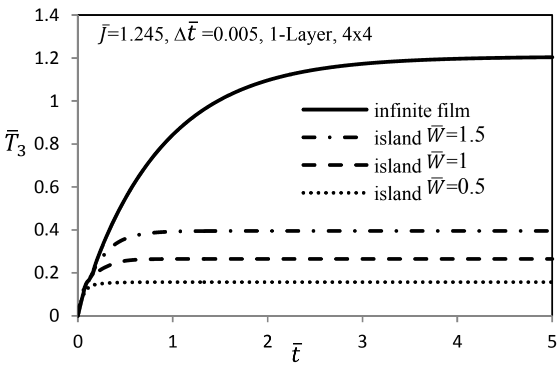

(a)

LOCATION B

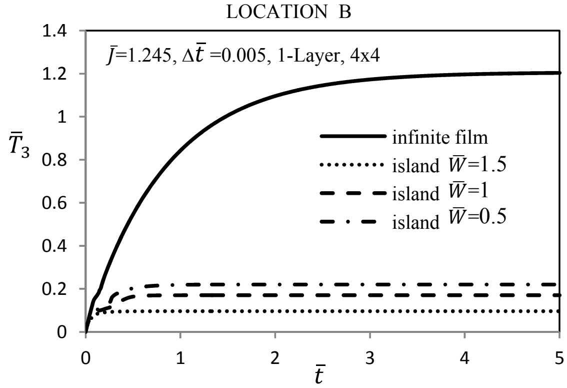

(b)

Figure 3. Temperature evolution in single-layer thin film with respect to time at (a) the location A & (b) location B for different island sizes.

The Figure 4 displays the thermal response of a 3-layer and a single layer SMA layer for $\overline{w} = 1$ at $\bar{t} = 5$, along a line from the bottom to the top of the island and running through its center. The spatial temperature profile is almost identical for the 3-layer and the single layer model, with a noticeable but small difference in Layer 1. Finally, the contour plot of the temperature profile for three different sizes of the SMA islands is presented in Figure 5 at $\bar{t} = 5$. As expected, the temperatures are higher towards Layer 1 and lower towards Layer 3, in all three cases. Further, the temperatures in the entire island for $\overline{w} = 0.5$ is considerably lower than the temperatures for $\overline{w} = 1.5$. While a smaller size translates to lower temperatures, this reduction is expected to be mitigated if a periodic structure of SMA islands is used. We plan to report results on periodic structures in the near future.

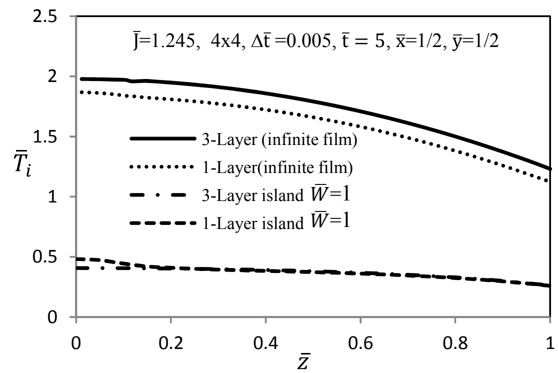

Figure 4. Temperature evolution in single-layer and three-layer thin film along the film thickness for infinite film and a thin film island with $\bar{W}$ = 1.

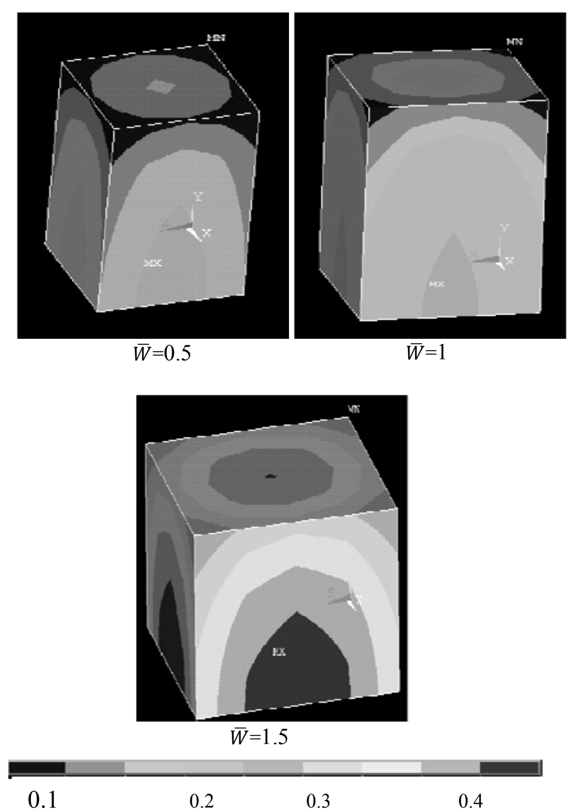

Figure 5. Contour plot of temperature variation on the island structure for different island sizes, $\bar{W}$= 0.5, 1 and 1.5 respectively. Here, the number of in-plane elements are 4x4, $\Delta\bar{t}$ =0.005, $\bar{t}$ = 5.

ISBN: 978-988-19252-6-8
ISSN: 2078-0958 (Print); ISSN: 2078-0966 (Online)

References

[1] Fu, Y., Du, H., Huang, W., Zhang, S., Hu, M., "TiNi-based thin films in MEMS applications: a review", Sensors and Actuators A (Physical), A112 (2-3), 395-408 (2004).

[2] Bhattacharyya, A., Ozturk, M.M., "Thermal response of infinitely extended Nickel-Titanium shape memory alloy thin film with variable material properties", SPIE Smart Structures/NDE (Conference: Behavior and Mechanics of Multifunctional Materials and Composites VII, 10-14 March 2013, San Diego, CA, Vol.8689 (to be submitted).

[3] Lee J.W., Thomas B. And Rabiei A., 'Microstructural study of titanium-palladium-nickel base thin film shape memory alloys', Thin Solid Films, 500, 309-315 (2006).

[4] Faulkner M.G., Almaraj J.J. & Bhattacharyya A., 'Experimental determination of thermal and electrical properties of NiTi shape memory wires', Smart Materials & Structures, 9, 632-639 (2000).

[5] Boyd, J.G., Lagoudas, D.C., "A thermodynamical constitutive model for shape memory materials", International Journal of Plasticity: Part I. The monolithic shape memory alloy, 12(6), 805-842.